Formation and Magnetotransport of Co/Pt Nano-Contacts through AlOx Barrier

	あるまはどうい　むふた　けーおー
氏　　名	Al-Mahdawi　Muftah K.O.
研究科，専攻の名称	東北大学大学院工学研究科（博士課程）電子工学専攻
学位論文題目	Formation and Magnetotransport of Co/Pt Nano-Contacts through AlO_x Barrier (AlO_x酸化物バリア層中へのCo/Ptナノ接点の形成と磁気輸送に関する研究)
論文審査委員	主査　東北大学教授　佐橋　政司 東北大学教授　大野　英男　　東北大学教授　白井　正文 教授　土井　正晶（東北学院大学）　教授　今村　裕志（産業技術総合研究所）

論 文 内 容 要 約

In this dissertation, I report on the formation and magnetotransport properties of Co/Pt nano-contacts through ultra-thin AlO_x Nano-Oxide-Layer (NOL) made by ion-assisted oxidation of 1–2-nm Al layer. The Co/Pt nano-contact (NC) formation was studied by conductive atomic force microscopy (cAFM) (ch. 4), conduction spectroscopy of electron-phonon interaction at nano-contacts (ch. 6), and transmission electron microscopy (ch. 6). The results suggest that AlO_x forms nano-holes (1–2 nm in diameter) during oxidation that are filled with Pt from top. The metallic property of NCs is reproducibly obtained when using Pt compared to CoFe alloys. The electrocatalytic properties of Pt are probably the reason behind this enhancement (ch. 5). The large spin-orbit coupling of Pt, enhanced at confined NC structure, is expected to show interesting effects. Current-perpendicular-to-plane anisotropic magnetoresistance (AMR) of the film stack Co/AlO_x -NOL/Pt was measured (ch. 7). Due to the random nature of NCs formation, Al contamination in NCs would reduce SOC considerably, and provide short paths to the purer Co/Pt NCs. Depending on the purity of NCs from Al contamination, we observed up to 29% AMR ratio at room temperature. An anomaly in resistance around 150 Kelvins was consistently observed, which can be attributed to presence of antiferromagnetic CoO at NCs. The effect of electric field on magnetic moments was studied, and signs of electrically-driven torques on magnetic moments were observed (ch. 8). In total, 9 chapters are presented.

Chapter 1: Introduction.

The interplay between charge and spin of transport electrons and manipulation thereof has generated interest in the past two decades, especially in metallic multilayers, that manifested in applications of non-volatile storage like hard-disk drive reading heads and magnetic random access memories. Most of magnetoelectronic devices depend on the presence of spin texture in Ferromagnet(FM) / Spacer / Ferromagnet multilayer geometries. On the other hand Spin-Orbit Coupling (SOC), that couples the spin of transport electrons to local crystal, can be used to make magnetoelectronic devices based on single FM layer. The most famous is the Anisotropic Magnetoresistance (AMR) in bulk 3d-transition ferromagnetic metals or alloys. Due to strong SOC, the Density Of States (DOS) can change depending on magnetization direction. In ballistic transport systems, the DOS controls the resistance or conductance directly, leading to AMR in both tunneling junctions and ballistic NCs [Park *et al.*, Phys. Rev. Lett., **100**, 8, 087204 (2008); Bolotin et al., Phys. Rev. Lett., **97**, 12, 127202 (2006)]. But in experiments reported up to now, AMR was observed only at low temperature (< 30K), even though room-temperature AMR effects are expected [Shick *et al.*, Phys. Rev. B, **73**, 2, 024418 (2006)]. NCs through AlO_x insulating spacer (Fig. 1) are stable even above room temperature, but up to now only FM NCs have been studied [Takagishi *et al.*, J. Appl. Phys., **105**, 7, 07B725]. The prospects of using such a structure for investigation of SOC-induced effects is explored in this research.

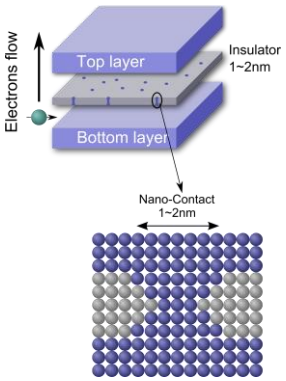

Fig. 1: Structure of NCs through AlOx

Chapter 2: Objectives and synopsis.

CPP magnetoelectronic devices based a single ferromagnetic (SFM) layer have been less explored than their textured counterparts (with two or more FM layers). They pose interesting problems in basic characterization and physics, as most SFM devices depend phenomena related to spin-orbit coupling. Also, they have potential applications because using a single FM layer allows a reduced element size compared to multilayer elements. The involved effective field of SOC are large (1–10 T per 10^8 A/cm^2 order of magnitude [Miron *et al.*, Nat. Mat., **9**, 3, 230 (2010)] which, in case of spin-orbit torque generation, can provide high frequency oscillations of magnetization (on order of 100 GHz). Thus, in this work I tried to develop ballistic Co/Pt NCs through AlO_x-NOL barrier and measure magnetotransport properties within. The primary objectives of this work are to experimentally:

- Make Co/Pt nano-contacts through AlO_x barrier, using the self-organized process of ion-assisted oxidation,
- Characterize the formation of Co/Pt NCs,
- And study the magnetotransport properties through Co/Pt NCs.

Chapter 3: Experimental methods.

The experimental flow of this work starts with sputter thin-film deposition of multilayer Ru 2/Co 2/AlO_x-NOL/Pt 7/Ru 0 or 5 over an electrode layer (Thickness in nm). The electrode layer is Ta 5 (sticking-layer)/Cu 285 or 200/Ta 30, which was chemo-mechanically planarized afterwards for smoothness. The substrate is a 1cm-by-1cm thermally-oxidized Si substrate with 200-nm SiO_2. Nano-Oxide Layer (NOL) was prepared by Ion-Assited Oxidation method, by bombarding the surface of 1.3-nm-thin metal Al with 65 eV Ar^+ ions, in the presence of 10^{-2} Pa oxygen atmosphere. This energy-assisted oxidation of Al is thought to form AlO_x grains with nano-holes in between them [Shiokawa *et al.*, IEEE Trans. Mag., **47**, 10, 3470 (2011)]. One set of samples after formation of NOL and before deposition of Pt was transferred *in situ* via transfer tube to cAFM chamber. Other Pt-capped samples were micro-fabricated into CPP pillar geometry, then resistance was measured by 4-wire method at either a Quantum Design PPMS or a home-made setup equipped with a helium cryostat. One of the film samples was sent to MST foundation for cross-sectional transmission electron microscopy.

Chapter 4: Co/AlO_x-NOL surface analysis by cAFM.

In this chapter, the formation of AlO_x-NOL by IAO-method over Co is investigated by cAFM. Upon contact of a semiconducting tip with a metallic film, a Schottky barrier is formed. The built-in potential (V_{bi}) of the junction, determined from the rectifying I-V curves, is the difference of work functions of the semiconductor and metal. Because the exact characteristics of cAFM tip (dopant density, acceptor and donor levels) are not known, each tip was calibrated for built-in potential over known material films (Co and Al). The difference of V_{bi} for Al and Co was 0.787 eV, which is close to the difference between reference values of Co and Al work functions. After calibration, using the same tip, unknown metals at AlO_x-NOL conductive paths were determined to be both Al and Co. So there is a distribution of pin-holes and FM-holes. When the mapping of V_{bi} was extended to the whole scan area (Fig. 2), Co paths constituted 20% of the total conductive paths area.

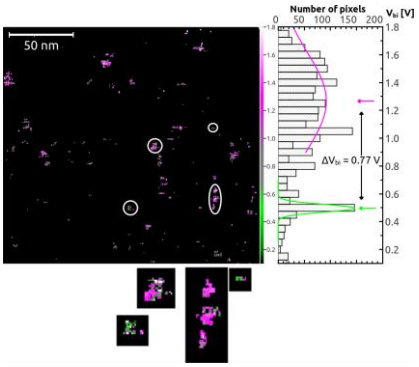

Fig. 2: V_{bi} scan of Co/AlO_x-NOL

Chapter 5: Effect of Pt top-layer on Co/AlO_x-NOL.

In this chapter, the effect of Pt top layer on Co/AlO_x with different IAO exposure times was studied. Pt is famous in use as catalysis. It has been shown that Pt can reduce oxidation states of Co and AlO_x [Zsoldos *et al.*, J. Phys. Chem., **95**, 2, 798 (1991)]. Also, Pt electrodes helped formation of conductive paths through metal oxide barriers more reliably [Tan *et al.*, Appl. Phys. A, **103**, 2, 293 (2011)]. Film with 30 sec IAO exposure a low RA product (0.08–0.18 Ωμm^2), with metallic-type conduction. Longer IAO time sample had much larger RA products. Also, when applying large bias, bi-stable switching of resistance was observed. This indicates that Pt has electro-catalytic properties that work to reduce oxidized Al or Co in AlO_x-NOL.

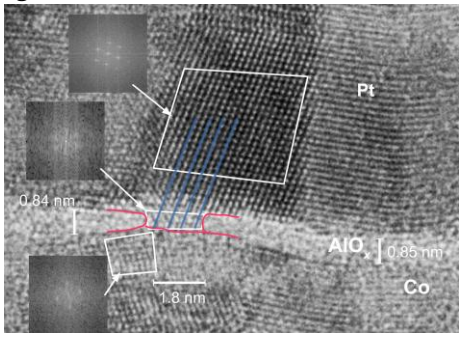

Fig. 3: TEM image of a Co/Pt NC through AlO_x-NOL

Chapter 6: Characterization of Co/AlO_x-NOL/Pt with short IAO time: CPP conduction and TEM imaging.

In this chapter, composition of metallic NCs in Co/AlO_x-NOL/Pt was investigated. Using the low-temperature dependence of zero-bias resistance and d^2v/di^2-bias spectrum, the dominant NCs in a single pillar is shown to vary between Al and Pt. Transmission electron micrograph also revealed what seems to be Pt contact to Co through AlO_x (Fig. 3).

Chapter 7: Current-perpendicular-to-plane anisotropic magnetoresistance of Co/Pt nano-contacts.

In this chapter, results of anisotropy in resistance depending on the relative angle between magnetization and current passing perpendicularly through Co/Pt NCs are reported. Al-NCs-dominant CPP pillars showed low AMR ratios (< 0.1%), whereas Pt-NCs-dominant pillars of the same substrate showed larger AMR ratios (> 0.5 %), with one of the pillars showing 30% AMR ratio (Fig. 4a). This AMR is from the change in local DOS of Pt NCs when the induced magnetization direction rotates relative to the current, and shows a Curie-Weiss-like dependence ($\propto B/T$). The temperature dependence of AMR ratio showed an increase with lowering temperature, but below 150 K AMR ratio is largely reduced (Fig. 4b). We attribute this reduction to pinning of Pt moments in-plane by a competition of FM coupling with Co and anti-FM coupling with CoO below the blocking temperature of CoO (T_B = 150K) (Fig. 5) [Sahashi *et al.*, IEEE Trans. Mag., **43**, 9, 3668 (2007)].

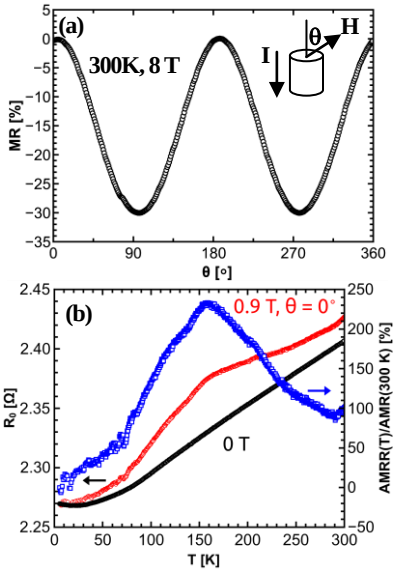

Fig. 4: (a) AMR-θ dependence. (b) AMR-temperature change.

Chapter 8: Towards a spin-orbit-torque oscillator.

In [Manchon, Phys. Rev. B, **83**, 17, 172403 (2011)], SOC at interfaces can work as a spin-density source thus exerting a torque on magnetic moments. On this chapter, we explored the existence of electrically driven torques at Co/Pt NCs, by measuring the change in *dv/di*-θ curve when the dc bias polarity is changed. Depending on bias polarity, the AMR curve features reversed around 180° (Fig. 6). For a plus (negative) bias the curve is broadened around 270° (90°), indicating a torque that works to stabilize the magnetic moment in in-plane direction dependent on bias. For estimation of this torque (effective field) order of magnitude, for ±30-mV bias, resistance differs from $cos(2\theta)$ by 30° at maximum. Using a simple vector relation, the resulting field can be estimated to be 6.2 T per 4×10^7 A/cm^2 (1.5×10^{-7} T·cm^2/A), assuming that the current flows uniformly in the whole pillar area. Including the concentration of current in NCs and the existence of many "dead" NCs will reduce this number by an order or two of magnitude. As a reference, the estimated Rashba-SOT field in Pt/Co/AlO$_x$ multilayer was on order of 0.1×10^{-7} T·cm^2/A [Miron *et al.*, Nat. Mat., **9**, 3, 230 (2010)], which has a similar order of magnitude to the one observed here.

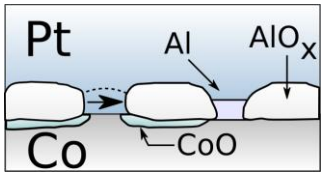

Fig. 5: Induced moments at Pt NCs are pinned by modulated FM/AFM coupling

Chapter 9: Conclusions and further directions.

In this chapter, final conclusions are outlined, and further directions are summarized. Kelvin-probe force microscopy is proposed as a better method to analyze the work function of NC materials. Also, provisions for comparison with small SOC materials are suggested.

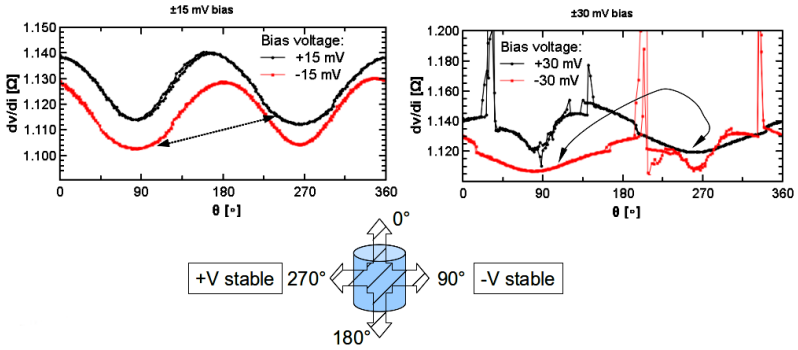

Fig. 6: Bias dependence of *dv/di*-θ, under 5 K and 8 T conditions.